

FPC FOR RIKEN QWR

K. Ozeki[†], O. Kamigaito, N. Sakamoto, K. Suda, and K. Yamada,
 RIKEN Nishina Center, Wako, Japan

Abstract

In RIKEN Nishina Center, three cryomodules which contain ten SC-QWRs in total (4 + 4 + 2) were constructed, and beam supply has been started since last year. The FPCs for RIKEN QWR have a disk-type single vacuum window at room-temperature region. A vacuum leakage occurred at one FPC, after 4th cool-down test. In addition, second vacuum leakage occurred at another FPC, after starting beam supply. A dew condensation at air side of vacuum window may degrade the brazing of vacuum window. In order to prevent a dew condensation and to restore damaged FPCs, Additional outer vacuum windows using machinable ceramics were designed and attached to the damaged FPCs. In this contribution, a structure of the FPC, troubles, provision for those troubles, and plan for reconstruction are reported.

INTRODUCTION

The RIKEN Heavy-ion linac (RILAC) [1] is used to supply intense beams for the synthesis of super-heavy elements (SHEs) [2], as well as used as an injector for following RIBF accelerator complex comprises four ring cyclotrons [3].

For the synthesis of new SHEs with atomic number greater than 118 and the production of radioactive isotopes for medical use, the RILAC has been upgraded (Fig. 1(a)). For an enhancement of the beam intensity, a new 28-GHz superconducting ECRIS (R28G-K) [4] was installed at the

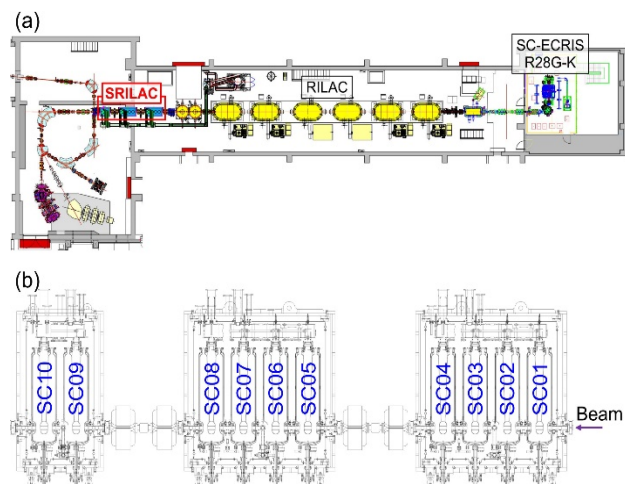


Figure 1: (a) An overview of RILAC upgrade. The R28G-K and SRILAC were installed at upmost-stream and downstream of RILAC, respectively. (b) A side view of SRILAC. Ten SC-QWRs are mounted in three cryomodules. Doublet quadrupole magnets are installed between each cryomodule.

[†] k_ozeki@riken.jp

uppermost-stream of RILAC. For an enhancement of the acceleration voltage, superconducting linac (SRILAC) [5-12] was installed at the downstream of RILAC. As shown in Fig. 1(b), the SRILAC comprises three cryomodules that mount ten superconducting quarter-wavelength resonators (SC-QWRs) in total.

A beam delivery to SHE research using R28G-K and SRILAC has started in June 2020.

STRUCTURE OF FPC

Schematic view and photograph of a fundamental power coupler (FPC) for SRILAC are shown in Figs. 2(a) and 2(b). It is a coaxial type of 39D and has a disk-type single vacuum window made of alumina ceramics (KYOCERA A479B) with a TiN coating. An outer conductor is made of copper-plated stainless steel and has an 80-kelvin thermal anchor. A thickness of copper plating is 30 μm . Residual resistivity ratio (RRR) of the copper plating is evaluated to be ~ 5 [13]. An inner conductor is made of an oxygen-free copper pipe. An assumed maximum RF power is 5 kW (continuous wave). The FPC is mounted on SC-QWR via 34D port located at the bottom of cavity. An

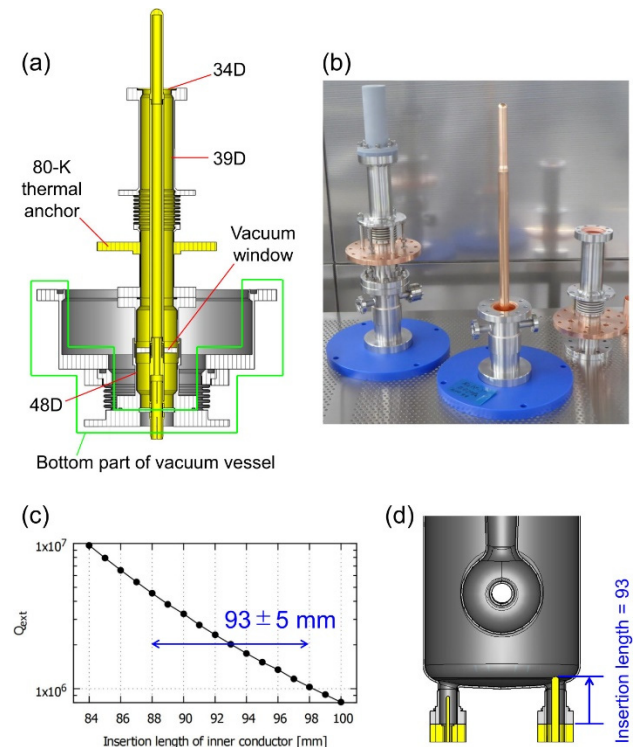


Figure 2: (a) Schematic view of FPC, including connecting portion with a vacuum vessel. (b) Photograph of FPCs. (c) Correlation between an insertion length of inner conductor and Q_{ext} , computed by CST MWS. (d) Schematic view with a standard insertion length of inner conductor.

insertion length of inner conductor can be varied by adjusting a length of bellows at the bottom part of vacuum vessel (Fig. 2(a)), without breaking the vacuum. The external quality factor Q_{ext} is tunable within the range of 1.0×10^6 to 4.5×10^6 with a stroke of ± 5 mm (Fig. 2(c)). Figure 2(d) shows a schematic view with a standard insertion length of the inner conductor.

HISTORY OF FPCS AND CRYOMODULES

The FPCs were delivered in sequence to RIKEN in 2018. A series of process of FPCs such as an ultrapure water rinsing, drying, particle removal, re-assembly, and RF process were all performed in ISO class-1 clean room [6]. Mounting of FPCs on QWRs were also performed in ISO class-1 clean room.

Assembly and installation of the cryomodules were completed in March 2019 [8]. Cryomodule operation was started from September, and cool-down tests were performed for several times. In November, a leakage from vacuum window of FPC mounted on SC05 (see Fig. 1(b)) occurred. It was an accident during warm-up process after fourth cool-down test, and at that time, a high-power RF test had not started yet. The SC05 was evacuated from air side of the FPC and preparations toward beam supply were continued.

We succeeded in first beam acceleration test in January 2020 and beam delivery to SHE research started in June [10]. In October, another leakage from vacuum window of FPC mounted on SC06 occurred. It was an accident during beam delivery, but there was no response at a FPC interlock system. The SC06 was also evacuated from air side of the FPC. Conditions of inside (air side of the vacuum window) of the remaining eight FPCs were inspected. As a result, a dew condensation and the degradation of both inner and outer conductor was confirmed (details are described below). A dry nitrogen gas was flown into both periphery of the vacuum window and inside of the inner conductor to prevent dew condensation, and the beam delivery was continued using remaining eight QWRs.

In May 2021, outer windows to restore damaged FPCs and prevent dew condensation were installed to the SC05 and SC06 and the RF power was successfully fed to both QWRs. Presently, all ten QWRs are used for beam acceleration.

DEGRADATION OF FPC

An inspection of inside of the FPCs were performed after the second vacuum leakage. An endoscope was inserted to the air side of vacuum window through a small hole at a supporting disk of the inner connector and inside conditions were observed. For some FPCs, condensed water was stood on the supporting disk. Part of the shot images are shown in Fig. 3. For all eight FPCs that were inspected (FPCs mounted on SC05 and SC06 were not inspected because the evacuation needed to be continued), spots after water evaporation on the vacuum window and the rust formations on inner and outer conductors were observed.

The vacuum window is metallized employing a molybdenum-manganese method, which is vulnerable to water. Although causes of vacuum leakage cannot be concluded yet, a galvanic corrosion induced by the condensed water might have degraded a brazing of the vacuum window.

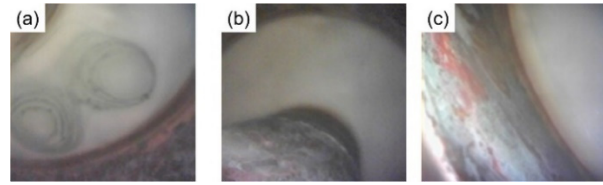


Figure 3: Shot images at the air side of vacuum window. (a) Spots after water evaporation on the vacuum window. (b)(c) Rust formations on inner and outer conductors.

TEMPERATURE DISTRIBUTION ESTIMATION

In a design phase of the FPC, we had a preconception that the temperature around the vacuum window is almost same as room temperature. But we recognized that it was wrong. We estimated the temperature distribution at a lower part of the FPC (from a bottom flange to 80-kelvin thermal anchor). A thermal conduction model at the lower part of FPC is shown in Fig. 4(a). In this model, the RRRs for bulk copper and copper plating were assumed to be 300 and 9, respectively.

Based on this model, thermal flows and temperatures at several points on FPC were calculated with various temperatures at the lowest points of inner and outer conductors (" T_{LP} " in Fig. 4(a)). As a result, as shown in Fig. 4(b), it was found that the temperature around the vacuum window was possibly cooled to nearly 0 degrees Celsius.

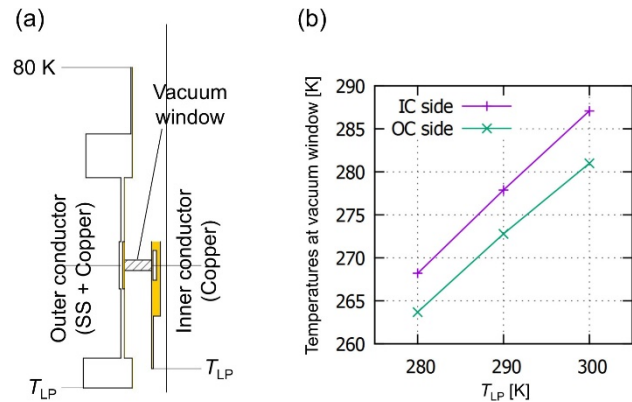


Figure 4: (a) Model of thermal distribution estimation. (b) Estimated temperatures at vacuum window. Temperatures at both inner and outer conductor side of vacuum window are shown.

INSTALLATION OF OUTER WINDOW

In order to restore damaged FPCs and prevent dew condensation around vacuum window of the FPC, we designed an outer window as shown in Fig. 5. A vacuum window of the outer window is made of a machinable nitride ceramics (Photoveel II). The outer window is vacuum-locked using O-rings and a region between the vacuum windows of FPC and outer window is evacuated.

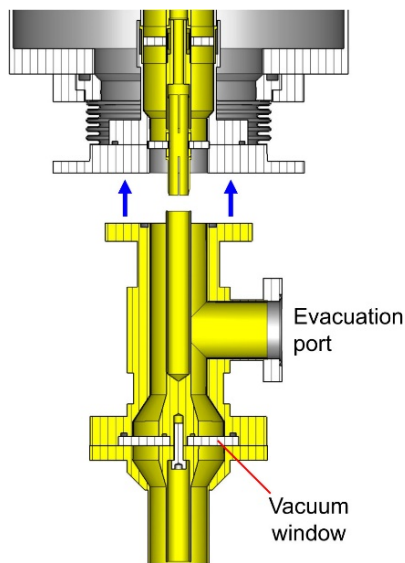


Figure 5: Schematic view of outer window.

As a first step, two sets of the outer windows were fabricated for usability tests. Two sets were connected together as shown in Fig. 6(a), and a vacuum lock test and RF test were performed. Figure 6(b) shows a setup for the RF test. Though there were some difficulties in achieving vacuum lock, the RF process was performed without any

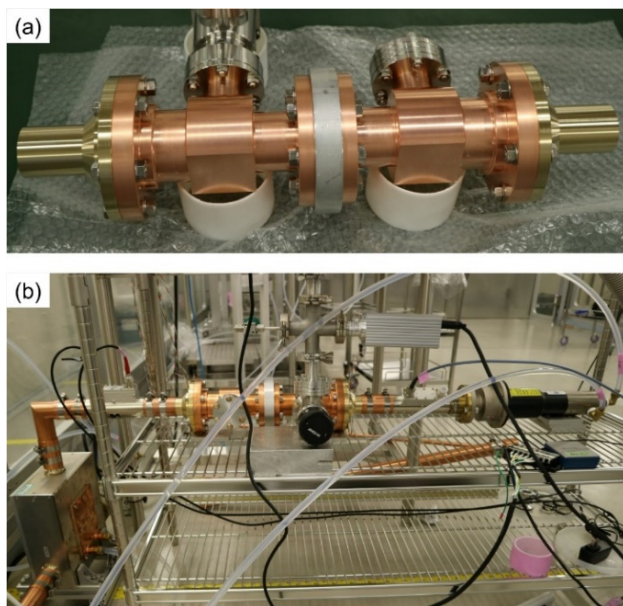


Figure 6 : (a) Connected two outer windows. (b) Setup for RF test of a pair of outer windows.

difficulties and RF power was fed up to 4 kW. After an usability of outer window was confirmed, these outer windows were installed to damaged FPCs and RF power was successfully fed to both SC05 and SC06. Owing to the installation of outer windows, a beam acceleration using all ten SC-QWRs was accomplished. Outer windows for remaining eight copplers are now in preparing.

FUTURE PROSPECTS

We plan to replace FPCs (components comprises inner conductor, vacuum window, and lower part of outer conductor, see Fig. 7(a)). In remodeling the component, we intended to improve thermal conduction at the lower part of outer conductor. Figure 7(a) shows its structure: the outer conductor between vacuum window and bottom flange is made of bulk copper.

We estimated the temperatures at vacuum window with this structure. The Model of thermal distribution estimation and estimated temperatures at inner and outer conductor side of the vacuum window are shown in Fig. 7(b). The temperatures at vacuum window that were almost same as room temperature were derived.

In addition to the improvement of thermal conduction, we plan to attach a heater around the vacuum window.

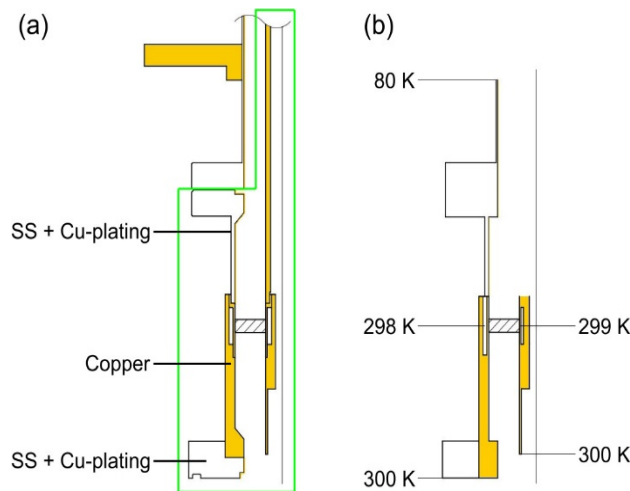


Figure 7: (a) Schematic view of remodeled FPC. The component to be replaced is indicated by green frame. (b) Model of thermal distribution estimation for remodeled FPC and estimated temperatures at vacuum window.

SUMMARY

In RIKEN Nishina Center, a cryomodule operation started in September 2019. Since then, the vacuum leakages from vacuum window of FPC occurred twice. A degradation of brazing of the vacuum window due to dew condensation around vacuum window is the most probable cause. The outer windows using machinable ceramics were installed to restore damaged FPCs and presently, a beam acceleration is performed using all ten SC-QWRs. We have a plan to replace FPCs with remodelled ones which can keep the temperature around vacuum window at room temperature.

REFERENCES

- [1] M. Odera *et al.*, “Variable frequency heavy-ion linac, RILAC: I. Design, construction and operation of its accelerating structure”, Nucl. Instrum. Methods Phys. Res., Sect. A, vol. 227, p. 187, 1984. doi:10.1016/0168-9002(84)90121-9
- [2] P. J. Karol *et al.*, “Discovery of the elements with atomic numbers Z=113, 115 and 117 (IUPAC Technical Report)”, *Pure Appl. Chem.*, vol. 88, p. 139, Feb. 2016. doi:10.1515/pac-2015-0502
- [3] Y. Yano, “The RIKEN RI beam factory project: A status report”, Nucl. Instrum. Methods Phys. Res., Sect. B, vol. 261, p. 1009, 2007. doi:10.1016/j.nimb.2007.04.174
- [4] T. Nagatomo *et al.*, “New 28-GHz Superconducting ECR Ion Source for Synthesizing New Super Heavy Elements of Z > 118”, in Proc. 23th International Workshop on ECR Ion Sources (ECRIS'18), Catania, Italy, Sep. 2018, pp. 53-57. doi:10.18429/JACoW-ECRIS2018-TUA3
- [5] N. Sakamoto *et al.*, “Construction Status of the Superconducting Linac at RIKEN RIBF”, in Proc. 29th Linear Accelerator Conf. (LINAC'18), Beijing, China, Sep. 2018, pp. 620-625. doi:10.18429/JACoW-LINAC2018-WE2A03
- [6] N. Sakamoto *et al.*, “Development of Superconducting Quarter-Wave Resonator and Cryomodule for Low-Beta Ion Accelerators at RIKEN Radioactive Isotope Beam Factory”, in Proc. 19th Int. Conf. RF Superconductivity (SRF'19), Dresden, Germany, Jun.-Jul. 2019, pp. 750-757. doi:10.18429/JACoW-SRF2019-WETEB1
- [7] K. Suda *et al.*, “Fabrication and Performance of Superconducting Quarter-Wavelength Resonators for SRILAC”, in *Proc. 19th Int. Conf. RF Superconductivity (SRF'19)*, Dresden, Germany, Jun.-Jul. 2019, pp. 182-187. doi:10.18429/JACoW-SRF2019-MOP055
- [8] K. Yamada *et al.*, “Construction of Superconducting Linac Booster for Heavy-Ion Linac at RIKEN Nishina Center”, in *Proc. 19th Int. Conf. RF Superconductivity (SRF'19)*, Dresden, Germany, Jun.-Jul. 2019, pp. 502-507. doi:10.18429/JACoW-SRF2019-TUP037
- [9] O. Kamigaito, K. Ozeki, N. Sakamoto, K. Suda, and K. Yamada, “Measurement of Mechanical Vibration of SRILAC Cavities”, in *Proc. 19th Int. Conf. RF Superconductivity (SRF'19)*, Dresden, Germany, Jun.-Jul. 2019, pp. 513-517. doi:10.18429/JACoW-SRF2019-TUP042
- [10] K. Yamada *et al.*, “Successful beam commissioning of heavy-ion superconducting linac at RIKEN”, presented at 20th Int. Conf. on RF Superconductivity (SRF'21), Virtual, June 2021, paper MOOFAV01, this conference.
- [11] K. Suda *et al.*, “New frequency-tuning system and digital LLRF for stable and reliable operation of SRILAC”, presented at 20th Int. Conf. on RF Superconductivity (SRF'21), Virtual, June 2021, paper WEPTEV013, this conference.
- [12] N. Sakamoto *et al.*, “Operation experience of the superconducting linac at RIKEN RIBF”, presented at 20th Int. Conf. on RF Superconductivity (SRF'21), Virtual, June 2021, paper MOPFAV005, this conference.
- [13] K. Kanaoka *et al.*, “Development for mass production of superconducting cavity by MHI”, in *Proc. ERL2015*, Stony Brook, NY, USA, Jun. 2015, pp. 72-74. doi:10.18429/JACoW-ERL2015-WEICLH2062